

Nonmonotonic dependence of intramolecular charge-transfer sidechain interactions for triazole containing phenylene-ethynylene grafted Co-Polyoxetane brushes

Masayuki Gon^{a,b}, Yoshiki Chujo^a, Olga Zolotarskaya^b, Kenneth J. Wynne^{b,*}

^a Department of Polymer Chemistry, Graduate School of Engineering, Kyoto University, Katsura, Nishikyo-ku, Kyoto, 615-8510, Japan

^b Chemical and Life Science Engineering, Virginia Commonwealth University, 601 West Main Street, Richmond, VA, 23284, USA

ARTICLE INFO

Keywords:

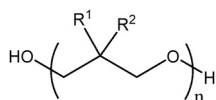
Brush polymer
Sidechain photoabsorption
Polyoxetanes

ABSTRACT

This research explores effects of introduction of the rigid phenylene ethynylene (PEy) moiety as a side chain in polyoxetanes. The synthesis of PEy-grafted polyoxetanes was carried out via Huisgen copper (I) catalyzed alkyne-azide cycloaddition. These polymers have a flexible main chain (low T_g polyoxetane) and rigid side chains (phenylene ethynylene). Compositions for copolyoxetanes with PEy and alkynyl side chains were determined by ¹H-NMR spectroscopy. Mole percents PEy, designated P-%, were P-21, P-44, P-69 and P-100. UV-VIS spectra for P-21, P-44, P-69, P-100 at 330 nm showed differentiation based on assignments to intramolecular charge-transfer (ICT) interactions between triazole and phenylene ethylene moieties. Interestingly, instead of a monotonic increase, absorption intensity is in the order P-69 ~ P-44 > P-100 > P-21. Low substitution and mainchain flexibility and account for P-21 having the lowest UV-VIS absorption at 330 nm. P-44 and P-69 have similar strong absorptions at 330 nm with overlapping curves. Steric effects culminate in P-100, which has the highest PEy content but a lower absorption at 330 nm than P-69 but higher than P-21. A model for optical absorptions for PEy copolyoxetanes is described that includes the effect of the rigid PEy side chain in decreasing molecular mobility.

1. Introduction

Polyoxetanes **1** have been prepared with a wide range of properties that are determined by side chains at the 3-position [1–7]. Introduction of side chain mesogens results in liquid crystalline polyoxetanes [2, 7–12] while semicrystalline polyoxetanes are obtained with two identical side chains such as poly(3,3-diethylloxetane) and poly(3,3-dimethylloxetane) [13–15]. Semicrystalline polyoxetanes are also found if one of the pendant groups is capable of hydrogen bonding [4].



Cationic ring-opening polymerization (ROP) has been used to prepare copolyoxetanes with a random distribution of comonomers [16, 17]. Unexpectedly, with a combination of fluororous and PEG-like comonomers, random or blocky copolyoxetanes were obtained depending on the order of monomer addition [18]. Copolyoxetanes **1** having repeat

units with quaternary (R^1) and PEG-like side chains (R^2) are water soluble and have amphiphilicity that mimics antimicrobial peptides (AMPS) with good human cell compatibility [19,20]. Recently, a ‘clickable’ and modular polyoxetane polymer platform was prepared consisting of acetylene-functionalized 3-ethyl-3-(hydroxymethyl)oxetane (EAMO) repeat units. This polyoxetane was conjugated with camptothecin, a topoisomerase I inhibitor, via a 3,3'-dithiodipropionic acid (DDPA) linker with a disulfide bond (S-S) extended by short-chain polyethylene glycol (PEG) to generate a polymer drug for glioblastoma multiforme therapy [21].

Low molar mass polyoxetane diols **1** with methyl (R^1) and fluororous (R^2) groups have atactic chain structures and low T_g 's. These viscous liquids can be employed as soft blocks for functional polyurethanes [22–24].

The present work explores introduction of triazole-linked rigid phenylene ethynylene (PEy) moieties as side chains in polyoxetanes. With a structure having benzene rings and π -conjugation, PEy exhibits interesting optical properties and is the subject for research in photonic materials [25–34]. Herein, we report PEy-grafted polyoxetanes

* Corresponding author.

E-mail address: kjwynne@vcu.edu (K.J. Wynne).

<https://doi.org/10.1016/j.polymer.2021.123569>

Received 13 November 2020; Received in revised form 15 February 2021; Accepted 18 February 2021

Available online 22 February 2021

0032-3861/© 2021 Elsevier Ltd. All rights reserved.

synthesized via Huisgen copper (I) catalyzed alkyne-azide cycloaddition [35,36]. These brush polymers have a flexible main chain (low T_g polyoxetane) and rigid side chains (phenylene ethynylene). The efficiency of click-coupling led to copolyoxetanes with molar ratios of PEy to alkynyl side chains by ^1H NMR that were close to reactant ratios. UV-VIS spectra were obtained, and unexpected optical properties were elucidated by molecular modeling and a study of thermal transitions by DSC.

2. Experimental section

Materials. 4-Iodobenzyl alcohol, phenylacetylene, bis(triphenylphosphine) palladium(II) chloride, triphenylphosphine, copper(I) iodide (CuI), 1,8-diazabicyclo[5.4.0]undec-7-ene (DBU), 1,1,4,7,7-pentamethyldiethylenetriamine (PMDTA), and organic solvents were purchased from Acros Organics. Triethylamine (Et_3N), diphenylphosphoryl azide (DPPA) and propargyl bromide (80% in toluene) were obtained from TCI America. Sodium hydride 60% dispersion in mineral oil, boron trifluoride diethyl etherate ($\text{BF}_3 \cdot \text{xEt}_2\text{O}$), 1,4-butanediol, and silica gel (pore size 60 Å, 70–230 mesh) were from Aldrich. 3-Ethyl-3-hydroxymethyl oxetane (EHMO) was a generous gift from Perstorp Polyols (Toledo, OH). (4-(Phenylethynyl)phenyl)methanol **3** was synthesized following the previously published procedure [37]. EAMO was prepared according to M. Jia's method [38]. Polymerization of EAMO was described by Zolotarskaya [39].

Synthesis of 1-(azidomethyl)-4-(phenylethynyl)benzene (4). THF (10 mL) and **3** (321 mg, 1.50 mmol) were placed in round-bottom flask equipped with magnetic stirring bar. DBU and DPPA were added to the mixture under N_2 . The reaction was carried out at room temperature for 24 h with stirring. Subsequently, the mixture was quenched by saturated, aqueous NH_4Cl and the organic layer extracted with CHCl_3 . The organic layer was washed with brine and dried over MgSO_4 . MgSO_4 was removed by filtration, and the solvent was evaporated. The residue was purified by flash column chromatography on SiO_2 (CHCl_3 as an eluent) to afford **4** (329 mg, 1.41 mmol, 94%) as light yellow crystals. $R_f = 0.84$ (CHCl_3). ^1H NMR (CDCl_3 , 600 MHz) δ 4.36 (s, 2H), 7.31 (d, 2H), 7.35 (m, 3H), 7.54 (m, 4H) ppm.

Synthesis of M1. EAMO (30.8 mg, 0.20 mmol), **4** (46.7 mg, 0.20 mmol), CuI (3.8 mg, 0.02 mmol), PMDTA (34.7 mg, 0.20 mmol), and THF (5 mL) were placed in round-bottom flask equipped with magnetic stirring bar. The reaction was carried out at room temperature for 20 h with stirring. After the reaction, the mixture was quenched with 28% aqueous NH_3 and the organic layer extracted with CHCl_3 . The organic layer was washed with brine and dried over MgSO_4 . MgSO_4 was removed by filtration, and the solvent was evaporated. The residue was purified by column chromatography on SiO_2 (gradient: from CHCl_3 to hexane/ $\text{EtOAc} = 1/1$ v/v and to EtOAc as an eluent) to afford **M1** (68.4 mg, 0.177 mmol, 88%) as a colorless liquid (Scheme 2). $R_f = 0.55$ (EtOAc). ^1H NMR (CDCl_3 , 600 MHz) δ 0.80 (t, 3H), 1.69 (q, 2H), 3.60 (s, 2H), 4.33 (d, $J = 5.8$ Hz, 2H), 4.40 (d, $J = 5.8$ Hz, 2H), 4.65 (s, 2H), 5.51 (s, 2H), 7.21 (d, 2H), 7.32 (m, 3H), 7.46 (s, 1H), 7.51 (m, 4H) ppm.

Post-functionalization of P(EAMO). P(EAMO) was click grafted with **4** to make brush polymers. A solution containing P(EAMO) (0.20 mmol of alkyne equivalent) in 5 mL of THF was prepared and addition of **4** was adjusted to achieve the following molar feed ratios of **4** to alkyne: 25/100, 50/100, 75/100, and 100/100. CuI (0.1 M amount of **4**) was added to the solution followed by addition of PMDTA (the same molar amount as **4**). The reaction mixture was stirred under N_2 for 20 h at room temperature. After the reaction, mixture was quenched by 28% aqueous NH_3 and the organic layer extracted with CHCl_3 , washed with brine and dried over MgSO_4 . MgSO_4 was removed by filtration, and the solvent was evaporated. The residue was purified by column chromatography on SiO_2 (gradient: from hexane/ $\text{CHCl}_3 = 1/1$ v/v to CHCl_3 as an eluent) to afford brush polymers P-#, where # indicates percentage of phenylene ethynylene brush units per polymer. According to ^1H NMR analysis, polymers P-21, P-44, P-69 and P-100 were obtained. ^1H NMR is typified by P-100 (CDCl_3 , 600 MHz): δ 0.72 (3H), 1.30 (br, 2H), 3.13 (br, 4H),

3.31 (s, 2H), 4.49 (br, 2H), 5.45 (s, 2H), 7.18 (s, 2H), 7.29 (s, 3H), 7.46 (br, 5H) ppm. Scheme 3 summarizes conditions and percent yields. Experimental details for preparation of P[(EAMO)(PEy)] copolymers are presented in Table S1.

Instrumentation. ^1H NMR spectra were recorded on either Varian Mercury-300 MHz or Bruker AVANCEIII 600 MHz instruments. ATR-IR spectra were obtained on a Nicolet Magna-IR 760 spectrometer by drop-casting on KBr pellets. Drop-casting on quartz substrates was used for Raman spectroscopy (Hariba LabRam HR Evolution; Lab Spec 6.2, 2014 software).

Gel permeation chromatography (GPC) was performed using a Viscotek GPC system equipped with a TriSEC triple detector. THF was the mobile phase with a flow rate of 1 mL/min. Universal calibration by polystyrene standards was used for determination of molar mass and polydispersity. Differential scanning calorimetry was performed on a TA-Q 1000 Series instrument (TA Instruments) with a heating rate of $10^\circ\text{C}/\text{min}$ and a cooling rate of $5^\circ\text{C}/\text{min}$ over the temperature range -90 to 100°C . Second scans are reported.

UV-VIS spectroscopy. UV-VIS spectra were obtained with a PerkinElmer Lambda 40 UV-Vis spectrophotometer. At an M1 concentration 1.0×10^{-5} M in CHCl_3 the peak absorbance was 0.4 with a cell path length of 10 mm (Figure S2). Molar absorptivity (ϵ) was difficult to estimate for the prepared polymers. Consequently, polymer solutions in CHCl_3 were prepared with absorbances close to M1 and normalized as shown in Figure S2 to obtain data shown in Fig. 3.

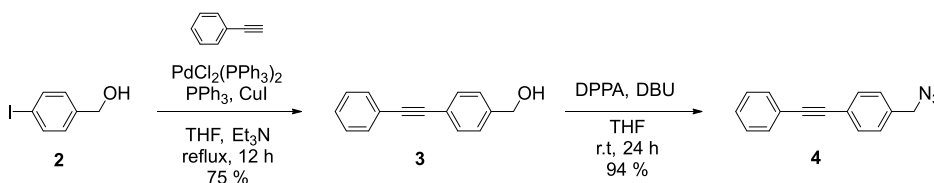
Polymer films were obtained by drop-casting dilute solutions on a quartz substrate at ambient temperature. The same preparation method was used for all samples to obtain data for elucidating differences. Peak absorbances at ~ 280 nm were normalized to 1.0 (Figure S3) to obtain the data shown in Fig. 5.

3. Results and discussion

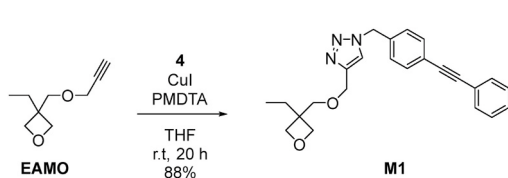
Synthesis. With reference to Scheme 1, Sonogashira-Hagihara coupling of 4-iodobenzyl alcohol **2** with phenylacetylene afforded compound **3** in 75% yield. The hydroxy group was converted to azide with DPPA and DBU giving compound **4** in 94% yield. EAMO [38] and P(EAMO) [39] were synthesized by reported methods. Molar masses for P(EAMO) were obtained by GPC: M_n (4,600), M_w (11,600) giving a PDI of 2.5. Model compound M1 was obtained by click reaction of EAMO and **4** in 88% yield (Scheme 2). M1 was used for ATR-IR and UV-VIS spectroscopy as a reference. (Phenylene ethynylene)-grafted polyoxetanes P-21, P-44, P-69, P-100 were synthesized by the reaction of **4** with the P(EAMO) alkyne moiety in molar feed ratios of 25/100, 50/100, 75/100, and 100/100 (Scheme 3). Polymerization was carried out under mild conditions to avoid degradation of the polymer main chain. GPC proved not suitable for characterization of copolymers because of decreased solubility with increasing side-chain substitution. However, adequate solubility permitted ^1H NMR spectroscopy, which was used to establish copolymer compositions. The ^1H NMR peak at 4.1 ppm for the CH_2 group adjacent to the acetylene moiety is designated 5 (Fig. 1, S1). This peak is prominent for P-21 due to 79 mol% EAMO side chains. The peak at 5.5 ppm, designated 7' is assigned to the CH_2 group adjacent to the aromatic moiety (Fig. 1, S1). This peak is strong in the spectrum of P-100 while the peak at 4.1 ppm is not detected. The integral of peaks 7' and 5 provided the mole ratio of (phenylethynyl)benzene to EAMO acetylene side chains.

The ^1H NMR spectrum for copolymers and P-100 have absorptions for 5' (4.5 ppm) that increase in intensity with increasing phenylene ethynylene content (Figure S1). Compared to other copolymers, the triplet-like absorption for P-44 is pronounced and likely reflects the presence of segments with different tacticities. The disorder wrought by different ways that phenylene ethynylene pendant groups are arranged along the main chain likely accounts for the broad T_g 's observed by DSC and is worthy of additional study.

Vibrational Spectroscopy. ATR-IR spectra were obtained to



Scheme 1. Synthesis of 1-(azidomethyl)-4-(phenylethynyl)benzene.



Scheme 2. Synthesis of compound M1.

confirm the presence of functionality (Fig. 2A). Compound 4 had a strong peak at 2094 cm^{-1} assigned to azide. P(EAMO) had a weak peak at 2116 cm^{-1} and a strong peak at 3290 cm^{-1} assigned to stretching vibrations of terminal alkyne group ($\text{C}\equiv\text{C}$) and ($\text{C}-\text{H}$), respectively. M1 had a weak peak at 2218 cm^{-1} that was identified as the stretching vibration of internal alkyne group between phenylene units and there were no peaks at 2094 cm^{-1} and 2116 cm^{-1} . In P-21, P-44, P-69, and P-100, the peaks for terminal alkyne (3290 and 2116 cm^{-1}) gradually decreased while the peaks for internal alkyne (2218 cm^{-1}) gradually increased with increasing substitution. No peak was observed at 2094 cm^{-1} which confirmed reagent 4 was not left in the polymer.

Small peaks in the vicinity of 1700 cm^{-1} were observed for all copolymers and P(EAMO). The absorption at 1700 cm^{-1} for P-44 almost reaches medium intensity. Such an absorption is characteristic of carbonyl groups, but the usually weak absorptions for P(EAMO) and copolymers suggests that these absorptions originate from combination bands arising from intense absorptions at $\sim 900\text{ cm}^{-1}$. A detailed investigation is outside the scope of the present investigation.

Raman spectra. To complement infrared spectroscopy, Raman spectra were obtained for films cast on quartz substrates (Fig. 2B). In the Raman spectra, the symmetric stretch of the internal alkyne group ($\text{Ph}-\text{C}\equiv\text{C}-\text{Ph}$) is observed as a strong peak at 2218 cm^{-1} for P-100, P-69 and P-44 and as a weak peak for P-21. The corresponding mode is extremely weak or not observed in the IR spectrum, which is consistent with the symmetric stretch being associated with a change in polarizability (Raman) rather than dipole moment (IR) [40]. Absorptions for the terminal alkyne group ($\text{C}\equiv\text{C}$, 2116 cm^{-1}) and terminal $\text{C}-\text{H}$ ($\text{C}-\text{H}$, 3290 cm^{-1}) are not observed in the Raman spectra.

UV-VIS spectra. UV-VIS spectroscopy was used to characterize CHCl_3 solutions of P-0 (P(EAMO)), P-21, P-44, P-69, P-100, and M1. The spectra shown in Fig. 3 were obtained by normalization based on M1 (Figure S2). UV-VIS spectroscopic data are collected in Tables S2-A, S2-B and S2-C.

In solution, P-0 exhibits negligible absorption from 250 nm to 500 nm as the alkyne moiety does not absorb in this region (Figure S2). The UV-VIS spectra of P-21, P-44, P-69, P-100, and M1 are similar to those for polyethers with bulky aromatic side chains reported by Nakano et al. [41] and related sidechain systems [42,43]. Strong absorptions from 280 to 305 nm (Fig. 3A) are assigned to phenylene ethynylene $\pi-\pi^*$ transition bands, while weak absorptions at 330 nm (Fig. 3B) are assigned to intramolecular charge transfer (ICT) bands arising from proposed interactions between 1,2-diphenylethyne and triazole moieties. This assignment is supported by the observation that the $\pi-\pi^*$ bands from 280 to 305 nm are not affected by the copolymer composition. If it were based on π -stacking, all bands would increase in intensity with increasing substitution (hyperchromicity). Interestingly, instead of a monotonic increase, the absorption intensity for PEy copolyoxetanes at 330 nm is in the order $\text{P-21} < \text{P-100} < \text{P-44} \sim \text{P-69}$. The ratios of the $280/320\text{ nm}$ absorptions are: P-21, 36; P-44 and P-69, 17 and P-100, 23,

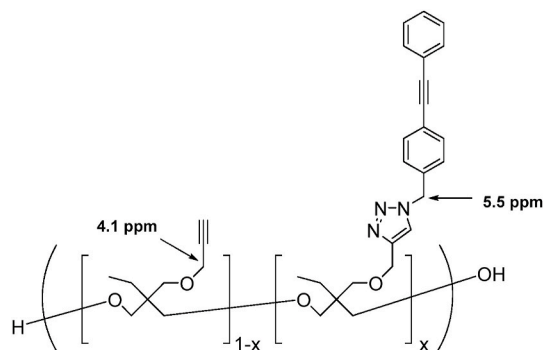
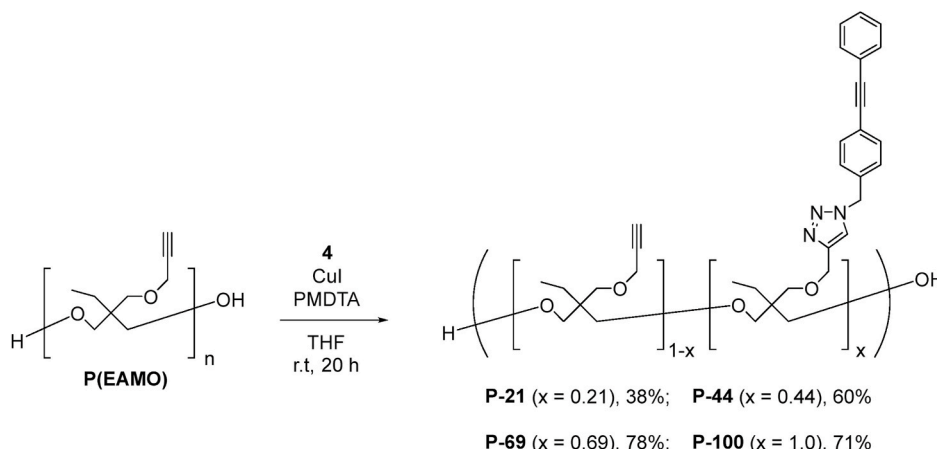


Fig. 1. Methylene groups are indicated for determination of co-monomer ratios by ^1H NMR spectroscopy.



Scheme 3. Synthesis of PEy copolymers from P(EAMO).

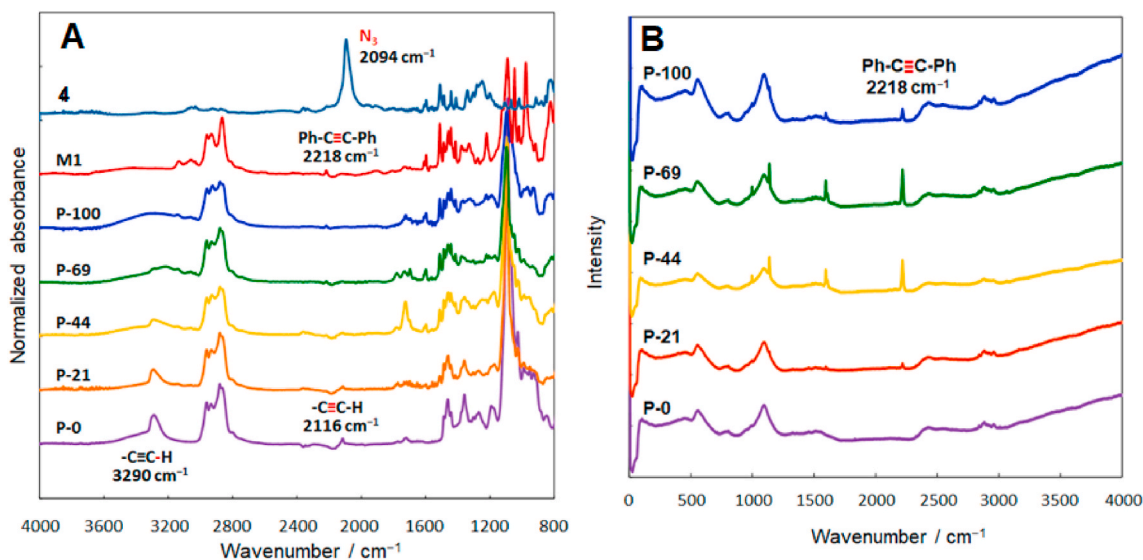


Fig. 2. A. ATR-IR spectra and B, Raman spectra of copolymers and P-0 (P(EAMO)).

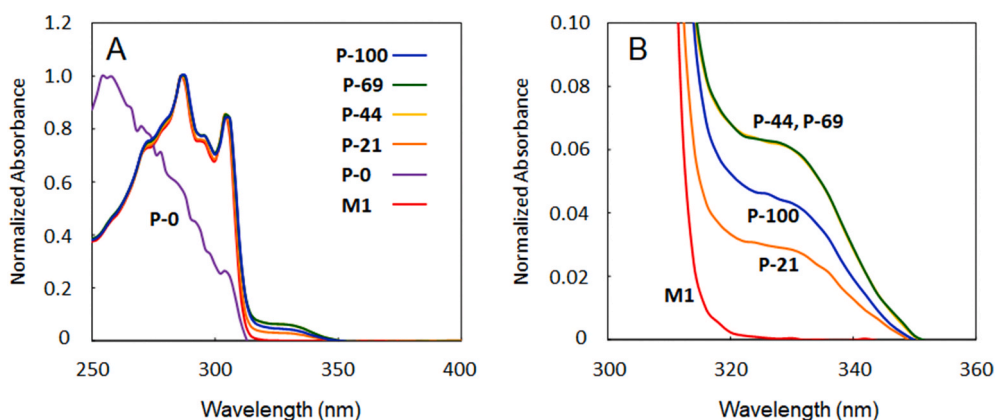


Fig. 3. UV-VIS spectra in CHCl_3 solution. A. 250–400 nm with normalization at peak maxima; B. 300–360 nm.

reflecting the relative increase of the ICT band (to P-44), leveling off (P-69) and decrease for P-100.

A schematic model for this finding is proposed in Fig. 4. Although ICT interactions are driven enthalpically, chain flexibility, chain structure and low substitution result in a low probability for interactions for

P-21. Compared to vinyl dibenzofulvene (DBF) π -stacked oligomers which have side chains occurring every other main chain atom [44], only one of every four mainchain atoms in PEy copolyoxetanes can bear a PEy side chain. Partial substitution for copolymers P-21, P-44 and P-69 further reduces the PEy side chain occurrence. Thus, it is interesting that

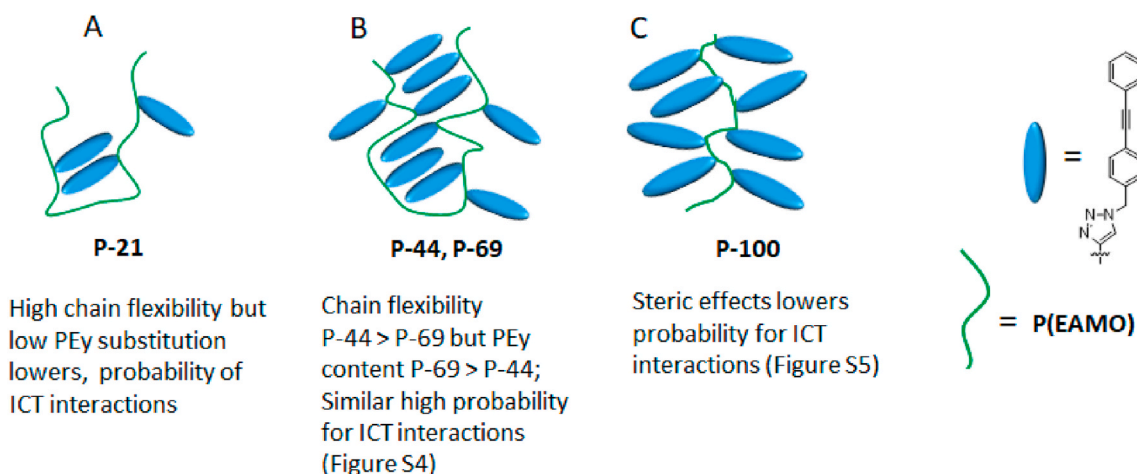


Fig. 4. Proposed mechanism for changes in UV-VIS spectra for phenylene-ethynylene grafted co-polyoxetanes.

P-21 has a UV-VIS absorption at 330 nm at all, considering that the frequency of PEy side chain occurrence could be as low as one for every 16 main chain atoms, depicted in Fig. 4A. This finding favors the proposed intramolecular charge transfer (ICT) bands.

P-44 and P-69 have similar absorptions at 330 nm with overlapping curves in Fig. 3B. The increased absorption for P-44 compared to P-21 is ascribed to increased ICT interactions due to increased PEy content. This argument fails to account for the equivalent absorption for P-69 at 330 nm compared to P-44. Rather, the onset of steric interactions and chain stiffness is proposed to account for this equivalence. That is, enthalpically driven ICT interactions are mitigated by increased steric effects driven by the bulky PEy side chain. Steric effects culminate in P-100, which has the highest PEy content but a lower absorption at 330 nm than P-69. Still, P-100 has a more intense absorption at 330 nm than P-21, so higher PEy content favors ICT interactions despite unfavorable steric effects.

Chem3D structures were obtained for additional insight into the relative order of UV-VIS absorptions. Figure S4 shows a representative structure for a copolyoxetane 10-mer with alternating PEy and EAMO side chains. Interestingly, several runs resulted in propinquity of PEy moieties noted by green arrows. This orientation favoring intramolecular ICT interactions depicted in Fig. 4B was found in multiple simulations. Figure S5 shows a representative Chem3D structure for a polyoxetane homopolymer 10-mer with PEy side chains. Multiple simulations failed to show orientations of PEy moieties favoring ICT interactions. Rather, aromatic PEy groups had orientations at odd angles disfavoring interactions supporting the model shown in Fig. 4C. Thus, modeling supports the non-intuitive higher UV-VIS absorptions attributed to intramolecular charge transfer (ICT) bands for P-44 and P-69 compared to P-100.

Spectra for films are shown in Fig. 5. The overall order P-21 < P-100 < P-44 ~ P-69 is not changed. However, the relative intensities for PEy copolyoxetanes P-69 and P-44 increase from ~0.06 in solution to ~0.11 in thin films (Tables S2 and S3). This doubling of intensity stands in contrast to the decreased intensity for P-100 from 0.043 in solution to ~0.034 in the thin film (Fig. 3, Tables S2 and S3).

The increased intensities for P-44 and P-69 in films indicates there is a stronger contribution from intermolecular ICT interactions in the condensed state compared to solutions (Tables S2 and S3). This is an interesting result, but given the unknown tacticity of the copolymers we can only speculate on the origin of this phenomenon. We note the unexpectedly lower relative absorption for P-100 in the thin film compared to solution (Tables S1, S2 and S3). This finding is attributed to steric effects that are apparently amplified in the condensed state and act to decrease ICT interactions.

Differential Scanning Calorimetry. Independent of processing, P-0, copolyoxetanes and P-100 form optically transparent films. DSC

thermograms were obtained to investigate the effect of increasing PEy content on T_g . P-0 has a sharply defined T_g at -35.3°C that is characteristic of a homopolymer. Increased substitution of the bulky PEy side chain results in a predictable trend toward higher glass transition temperatures that are in the range -5 to 23°C . With increased PEy content decreasing changes in heat capacities with increasing T_g are accompanied by broader transitions (Fig. 6). The endotherm for P-44 is particularly broad; there may be a low temperature transition that would require further work for confirmation. Given the relatively narrow range of copolymer T_g 's which are below or near the UV-VIS measurement temperature it is unlikely that the trend in reduced molecular mobility contributes to the unexpected decrease in the thin film absorption attributed to ICT for P-100 at 320 nm.

Conclusion. EAMO [38] and P(EAMO) [39] were synthesized by reported methods. Molar masses for P(EAMO) were obtained by GPC: M_n (4,600), M_w (11,600) giving a PDI of 2.5. The reaction of 4 with the P (EAMO) alkyne moiety by click chemistry resulted in efficient grafting of phenylene ethynylene (PEy). Control of stoichiometry gave a series of polyoxetanes designated P-21, P-44, P-69 and P-100 for percent PEy (Scheme 3). Copolymer compositions were established by ^1H NMR spectroscopy using unique peaks for the respective side chains. UV-VIS spectroscopy revealed absorptions at 330 nm ascribed to side chain triazole-phenylene ethynylene ICT interactions by analogy with work of Nakano et al. on vinyl oligomers containing dibenzofulvene (DBF) side chains (Fig. 3B) [41,42].

Surprisingly, instead of a monotonic increase following PEy content, the absorption intensity at 330 nm is in the order P-21 < P-100 < P-44 ~ P-69. A model for this finding is based on steric effects that decrease triazole-phenylene ethynylene interactions for fully substituted P-100 (Fig. 4). Molecular modeling (Chem3D) for a 50-50 copolymer showed orientations favoring intramolecular interactions between 1,2-diphenylethyne and triazole moieties in multiple simulations (Figures S3, 4B). However, multiple simulations failed to show orientations of PEy moieties favoring triazole-phenylene ethynylene interactions for a P-100 model. Rather, PEy groups had orientations at odd angles disfavoring interactions as depicted in Fig. 4C. Thus, modeling supports the non-intuitive higher UV-VIS absorptions for P-44 and P-69 compared to P-100.

Absorbance intensity for thin films follows the same relative order found in solution but the absorbance at 330 nm doubles for P-44 and P-69. However, the absorbance intensity for P-100 is about 25% lower than that found in solution (Table S2). The decrease in the UV-VIS absorption at 330 nm for P-100 thin films correlates with intramolecular steric effects illustrated in Fig. 4C. Steric effects could well contribute to decreased interactions between 1,2-diphenylethyne and triazole moieties, but details remain to be investigated in future work. DSC for the copolyoxetanes and P-100 shows a relatively narrow 25°C range for

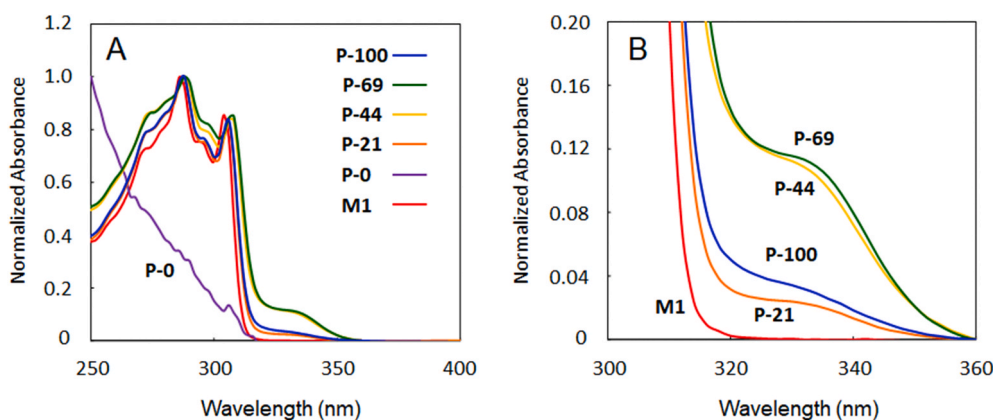


Fig. 5. UV-VIS spectra for copolymer films. A. 250–400 nm with normalization at 288 nm (maximum) and 360 nm (negligible absorbance); B. 300–360 nm; M1 spectrum was in dilute CHCl_3 .

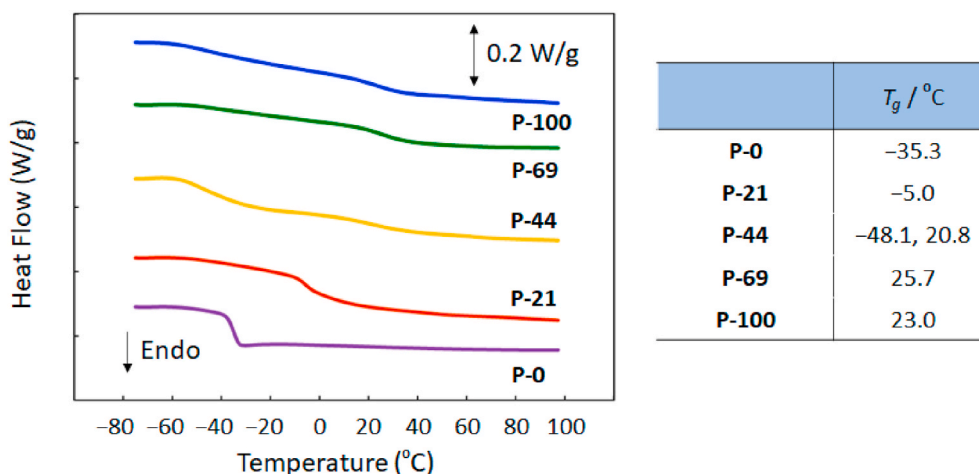


Fig. 6. DSC thermograms and T_g 's for PEy co-polyoxetanes; scan rate 10 °C/min.

T_g 's, which are characterized by broad transitions with low changes in heat capacity. From these data it seems unlikely that diminished macromolecular mobility alone reduces chances for interactions between 1,2-diphenylethyne and triazole moieties.

Declaration of competing interest

The authors declare that they have no known competing financial interests or personal relationships that could have appeared to influence the work reported in this paper.

Acknowledgements

K.J.W. thanks the National Science Foundation, Division of Materials Research, Polymers Program (DMR-1206259) and Biomaterials Program (DMR-1608022) and the School of Engineering Foundation for partial support of this research. MG thanks the Wynne group for their help in conducting this research during his tenure as a visiting scholar at VCU.

Appendix A. Supplementary data

Supplementary data to this article can be found online at <https://doi.org/10.1016/j.polymer.2021.123569>.

References

- [1] M.A. Gomez, E.D.T. Atkins, C. Upstill, A. Bello, J.G. Fatou, *Polymer* 29 (1988) 224.
- [2] Y. Kawakami, K. Takahashi, H. Hibino, *Macromolecules* 24 (1991) 4531.
- [3] H. Desai, A.V. Cunliffe, M.J. Stewart, A.J. Amass, *Polymer* 34 (1993) 642.
- [4] J.M. Parris, R.H. Marchessault, E.J. Vandenberg, J.C. Mullis, *J. Polym. Sci. B Polym. Phys.* 32 (1994) 749.
- [5] D. Takeuchi, Y. Watanabe, T. Aida, S. Inoue, *Macromolecules* 28 (1995) 651.
- [6] D. Takeuchi, T. Aida, *Macromolecules* 33 (2000) 4607.
- [7] Y.K. Yun, D.H. Ko, J.I. Jin, Y.S. Kang, W.C. Zin, B.W. Jo, *Macromolecules* 33 (2000) 6653.
- [8] Y.H. Lu, C.S. Hsu, *Macromolecules* 28 (1995) 1673.
- [9] Y. Kawakami, Y. Kato, *Polym. J.* 29 (1997) 775.
- [10] S.J. Cowling, K.J. Toyne, J.W. Goodby, *J. Mater. Chem.* 11 (2001) 1590.
- [11] K.N. Kim, Y.W. Kwon, C.W. Jang, M.J. Kim, T.K. Lim, J.I. Jin, *Liq. Cryst.* 34 (2007) 535.
- [12] L.C. Wu, C.C. Chen, C.H. Lin, *Polymers* 12 (2020).
- [13] E. Perez, M.A. Gomez, A. Bello, J.G. Fatou, *Colloid Polym. Sci.* 261 (1983) 571.
- [14] G.V.S. Henderson Jr., K.E. Hardenstine, C.J. Murphy, L.H. Sperling, G.E. Manser, *Polym. Mater. Sci. Eng.* 53 (1985) 801.
- [15] Y. Zheng, K.J. Wynne, *Polym. Mater.: Sci. Eng. Preprints* (2007) 362.
- [16] H. Cheradame, J.-P. Andreolety, E. Rousset, *Makromol. Chem.* 192 (1991) 901.
- [17] T. Fujiwara, U. Makal, K.J. Wynne, *Macromolecules* 36 (2003) 9383.
- [18] T. Fujiwara, K.J. Wynne, *Macromolecules* 37 (2004) 8491.
- [19] S. Chakrabarty, A. King, P. Kurt, W. Zhang, D.E. Ohman, L.F. Wood, C. Lovelace, R. Rao, K. Wynne, *J. Biomater. Sci.* 12 (2011) 757.
- [20] A. King, S. Chakrabarty, W. Zhang, X. Zeng, D.E. Ohman, L.F. Wood, S. Abraham, R. Rao, K. Wynne, *J. Biomater. Sci.* 15 (2014) 456.
- [21] J. Allen, J. Wang, O.Y. Zolotarskaya, A. Sule, S. Mohammad, S. Arslan, K.J. Wynne, H. Yang, K. Valerie, *J. Contr. Release* 321 (2020) 36.
- [22] U. Makal, T. Fujiwara, R.S. Cooke, K.J. Wynne, *Langmuir* 21 (2005), 10749.
- [23] P. Kurt, L. Wood, D.E. Ohman, K.J. Wynne, *Langmuir* 23 (2007) 4719.
- [24] S.S. Nair, E.J. McCullough, V.K. Yadavalli, K.J. Wynne, *Langmuir* 30 (2014), 12986.
- [25] J.D. Fox, S.J. Rowan, *Macromolecules* 42 (2009) 6823.
- [26] L. Jones, J.S. Schumm, J.M. Tour, *J. Org. Chem.* 62 (1997) 1388.
- [27] I.B. Kim, B. Erdogan, J.N. Wilson, U.H.F. Bunz, *Chem. Eur. J.* 10 (2004) 6247.
- [28] H. Li, D.R. Powell, R.K. Hayashi, R. West, *Macromolecules* 31 (1998) 52.
- [29] R.M. Meudtner, S. Hecht, *Angew. Chem. Int. Ed.* 47 (2008) 4926.
- [30] M.R. Pinto, K.S. Schanze, *Synthesis-Stuttgart* (2002) 1293.
- [31] T.M. Swager, *Acc. Chem. Res.* 41 (2008) 1181.
- [32] C.Y. Tan, E. Alas, J.G. Muller, M.R. Pinto, V.D. Kleiman, K.S. Schanze, *J. Am. Chem. Soc.* 126 (2004), 13685.
- [33] J.H. Wosnick, C.M. Mello, T.M. Swager, *J. Am. Chem. Soc.* 127 (2005) 3400.
- [34] S.M. Wu, M.T. Gonzalez, R. Huber, S. Grunder, M. Mayor, C. Schonenberger, M. Calame, *Nat. Nanotechnol.* 3 (2008) 569.
- [35] H.C. Kolb, M.G. Finn, K.B. Sharpless, *Angew. Chem. Int. Ed.* 40 (2001) 2004.
- [36] M.G. Finn, H.C. Kolb, V.V. Fokin, K.B. Sharpless, *Prog. Chem.* 20 (2008) 1.
- [37] T. Schabel, C. Belger, B. Plietker, *Org. Lett.* 15 (2013) 2858.
- [38] M.C. Jia, A.L. Li, Y.B. Mu, W. Jiang, X.B. Wan, *Polymer* 55 (2014) 1160.
- [39] O.Y. Zolotarskaya, Q. Yuan, K.J. Wynne, H. Yang, *Macromolecules* 46 (2013) 63.
- [40] K. Hashimoto, V.R. Badarla, A. Kawai, T. Ideguchi, *Nat. Commun.* 10 (2019) 4411.
- [41] M. Merlani, Z. Song, Y. Wang, Y. Yuan, J. Luo, V. Barbakadze, B. Chankvetadze, T. Nakano, *Macromol. Chem. Phys.* 220 (2019) 1900331.
- [42] T. Nakano, K. Takewaki, T. Yade, Y. Okamoto, *J. Am. Chem. Soc.* 123 (2001) 9182.
- [43] T. Nakano, *Polym. J.* 42 (2010) 103.
- [44] T. Nakano, T. Yade, *J. Am. Chem. Soc.* 125 (2003), 15474.